



RBF NEURAL NETWORK FOR CHAOTIC MOTION CONTROL OF COLLISION VIBRATION SYSTEM

SHUYU ZHOU*

Abstract. Aiming at the control problem of chaotic motion of a kind of collision vibration system with gap, a chaotic motion control of collision vibration system based on RBF neural network is proposed. Firstly, the system mechanical model and chaotic motion are introduced, and then a chaotic controller based on RBFNN is designed to control and simulate the chaotic attractor. The model information of the system is not used in the control method. In this paper, the model of the system is used only to generate the input / output data of the system, and it is not used for the design of the controller. The parameters of AHGSA algorithm are set as follows: the population size is 30, the maximum number of iterations is 100, G_0 , $a = 18$, and the proportional coefficient $P = 0.96$. Small disturbances are applied to the controllable parameter ω of the system to suppress the chaotic motion of the system and make the system tend to stable periodic motion. In order to more clearly show the control effect of chaotic motion, the chaotic motion is controlled when the system iterates 400 times. The results show that the chaotic motion can be quickly controlled to periodic 1-1 motion, the phase diagram is a closed curve, and there is a peak in the spectrum diagram. Chaotic motion can be quickly controlled as periodic 2-2 motion, the phase diagram is two closed curves, and two obvious peaks appear in the spectrum diagram. The proposed method can effectively control the chaotic motion of the system, and the expected target can be not only the fixed point of period 1, but also other periodic orbits.

Key words: collision vibration, chaotic motion control, RBF neural network, Chaos controller

1. Introduction. Collision vibration system with gap widely exists in practical engineering systems such as locomotives, vehicles and mechanical equipment. Its dynamic behavior is rich and complex (including bifurcation and chaos). Effectively controlling the chaotic behavior of this kind of system has important theoretical significance and engineering application value to ensure the safe service of the system [1]. However, due to the existence of collision behavior, the system speed will jump before and after collision, resulting in continuous but not smooth system displacement. This kind of system has non smooth nonlinear characteristics. Therefore, some dynamic theories and control methods suitable for smooth systems are difficult to be directly applied to such systems. The compliance control framework of teleoperation system based on RBF neural network is shown in Figure 1.1 [2]. In order to optimize the working effect, it is necessary to study the theory and method of chaotic motion control for collision vibration system [3]. In practical application, due to design, manufacturing or assembly errors and other factors, there will be gaps between parts in the mechanical system, resulting in collision and vibration between parts under external incentives [4].

2. Literature review. In view of this problem, Huynh, T. T. et al. firstly from the viewpoint of modern dynamical system, studied a unilateral constrained oscillator, analyzed the local bifurcation of periodic motion by using the central manifold theorem, and analyzed its chaotic motion by using the homoclinic phase cut condition [5]. Burdukovsky, I. et al. studied the two degree of freedom collision vibration system excited by simple harmonic force by numerical simulation method, and confirmed that it leads to chaos through period doubling waterfall [6]. Jaddi, N. S. et al. first proposed a strategy to control chaos, the famous OGY method, by using the sensitivity of chaotic system to parameter changes and the density of unstable periodic orbits of chaotic attractors [7]. Xu, Z. et al. proposed different improvement measures and further developed the OGY method [8]. Lian, HH et al. proposed the idea of state delay feedback control to control chaos. Due to non-smooth factors such as collision, impact and dry friction, the vector field will be non-differentiable or discontinuous, so that the traditional theory of smooth dynamical system cannot be directly used in non-smooth

*ChongQing Technology And Business Institute, Chongqing, 401520, China (Corresponding author, ShuyuZhou2@163.com)

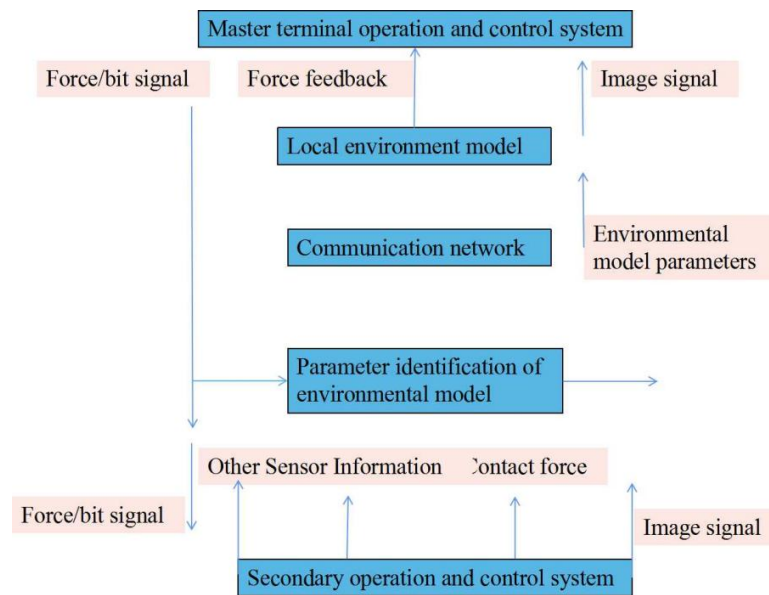


Fig. 1.1: Compliance control of teleoperation system based on RBF neural network

dynamical system, and some control methods for smooth dynamical system are no longer applicable in non-smooth dynamical system [9]. Due to the existence of collisions, the collision vibration system has non-smooth and strong nonlinear characteristics. Its complex and unstable dynamic behavior (such as chaotic behavior) will not only cause noise or wear of mechanical parts, but even endanger the safety of the system. For example, due to the existence of wheel rail gap, when the running speed of locomotive and vehicle is higher than the critical speed of locomotive and vehicle hunting motion, with the increase of running speed, the hunting motion will gradually deteriorate, the vibration displacement of each rigid body will become larger and larger, and finally there will be bifurcation phenomenon and chaotic operation state. Violent collision between wheel and rail will lead to the deterioration of locomotive and vehicle running performance. It may not only damage wheel sets and lines, but also cause derailment accidents. The flow of the vehicle collision vibration system is shown in Figure 2.1. Muthukumar, P. et al. proposed the control strategy of fitting Poincare map by experimental data and pole assignment by partition [10]. Congxu et al. localized the rub-collision mapping of the rotor near the rubbing track, and fitted the local mapping through experimental data, and controlled the chaotic motion of the rub-collision rotor system by variable delay feedback control method [11]. Qi, G. et al. proposed a new feedback control method that uses a small amplitude control signal to change the energy of a chaotic system to achieve the purpose of controlling chaos [12]. Wang, H. et al. used a piecewise linear absolute value function to obtain the control signal. In the actual control process, chaos control was performed by changing the damping coefficient [13]. Fan, J. et al. applied this method to a single-degree-of-freedom collision vibration system to control chaos [14]. Zotos et al. proposed a kind of single-degree-of-freedom collision oscillator position control strategy based on the feedback control idea [15]. E K ö se et al. Proposed chaos control strategy based on state variable predictive feedback and nonlinear delay feedback chaos control strategy for a class of single degree of freedom collision vibration system, and proposed parameter self-adjusting chaos control strategy for a class of two degree of freedom collision vibration system [16]. Zeng, H. B. et al. realized the control of chaotic motion of a class of single degree of freedom collision vibration system by 0GY method [17]. Kong, L. et al. realized the position control of a two-degree-of-freedom collision vibration system under asymmetric bilateral constraints based on feedback control ideas [18]. Zeng, Z. P. et al. realized the control of chaotic motion by changing the damping coefficient of a single degree of freedom collision vibration system. Most of the existing control methods for the chaotic motion of collision vibration systems require knowledge of the controlled system model. However, it is not easy to accurately model the actual engineering system. Unmodeled dynamics are always

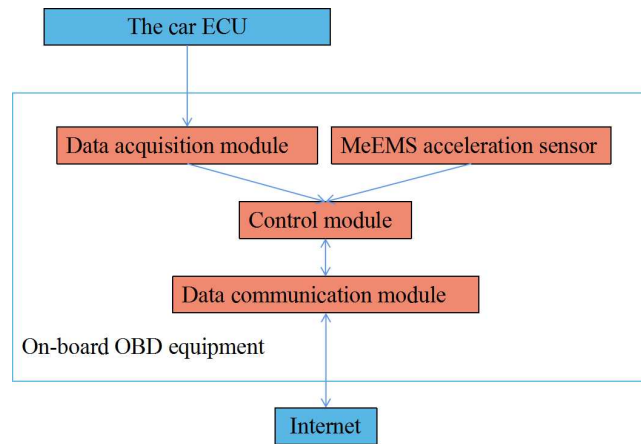


Fig. 2.1: Process of car collision vibration system

difficult to avoid, which makes it difficult to optimize the traditional control methods. The control performance [19]. On the basis of the current research, the chaotic motion control of the collision vibration system based on the RBF neural network is proposed. First, the system mechanics model and chaotic motion are introduced, and then the chaos controller based on RBFNN is designed, and the chaotic attractor is controlled and simulated. The model information of the system is not used in the control method. In this paper, the model of the system is used only to generate the input / output data of the system, and it is not used for the design of the controller.

The parameters of the AHGSA algorithm are set as follows: the population size is 30, the maximum number of iterations is 100, $G_0=130$, $a=18$, and the proportional coefficient $p=0.96$. A small disturbance is applied to the controllable parameter of the system ω to suppress the chaotic motion of the system and make the system tend to a stable periodic motion. In order to show the effect of chaotic motion control more clearly, the chaotic motion is controlled when the system is iterated 400 times. The results show that chaotic motion can be quickly controlled to a period of 1-1 motion, the phase diagram is a closed curve, and a peak appears in the spectrogram. The chaotic motion can be quickly controlled to a period of 2-2 motion, the phase diagram is two closed curves, and the spectrogram shows two obvious peaks. Simulation analysis shows that effective chaos control cannot be completed.

And when the number of hidden layer nodes increases, the nonlinear mapping ability of the controller is enhanced, and the intelligent algorithm optimizes the appropriate controller parameters, the control effect becomes better.

3. Methods.

3.1. System mechanics and chaotic motion. The control of chaotic motion of a collision vibration system with gap and a class of single degree of freedom collision vibration system with gap are studied. The mass is denoted by M , and its displacement is denoted by X . The mass and the left rigid constraint are connected by a linear spring with a stiffness of K and a linear damper with a damping coefficient of C . When the mass M is in the equilibrium position, the gap between it and the right rigid constraint is B . The simple harmonic incentive force acting on the mass is $Fsin(\Omega T + \tau)$.

If the collision duration is negligible, the differential equation of system motion is:

$$\begin{cases} M\ddot{X} + C\dot{X} + KX = Fsin(\Omega T + \tau), X < B \\ \dot{X}_+ = -R\dot{X}_-, X = B \end{cases} \tag{3.1}$$

where \ddot{X} , \dot{X} and X are the acceleration, velocity and displacement of the mass M . M , C , K are the mass of M , the damping of the linear damper and the stiffness of the linear spring respectively. \dot{X}_- , \dot{X}_+ is the instantaneous velocities before and after the collision between mass M and the right rigid constraint, respectively. R is

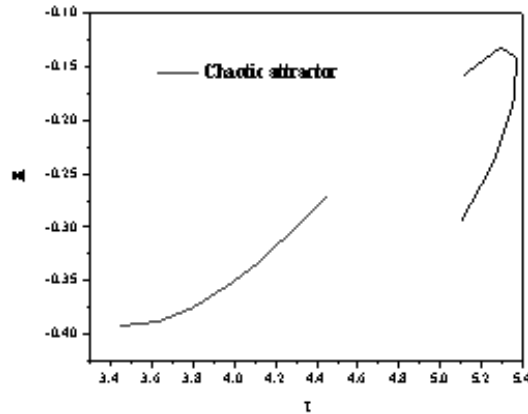


Fig. 3.1: Chaotic attractor

the coefficient of restitution. Without loss of generality, introduce the dimensionless quantity $x = \frac{XK}{F}, \zeta = \frac{C}{\sqrt{MK}}, \omega = \Omega\sqrt{\frac{M}{K}}, t = T\sqrt{\frac{K}{M}}, b = \frac{BK}{F}$ and carry on the dimensionless transformation to the Equation 3.1, and get:

$$\begin{cases} \ddot{x} + 2\zeta\dot{x} = x = \sin(\omega t + \tau), x < b \\ \dot{x}_+ = -R\dot{x}_-, x = b \end{cases} \quad (3.2)$$

where \dot{x}_-, \dot{x}_+ are the instantaneous velocities before and after the collision between the mass M and the right rigid constraint.

In order to study the evolution mechanism of system dynamics, the instantaneous cross-section σ after collision is selected, $\sigma = \{(x, \dot{x}, \theta) \in R^2 \times S^1 | x = b, \dot{x} = \dot{x}_+\}$, where $\theta = \omega t \text{ mod } 2n\pi$ is the Poincare cross-section, and the parameter that affects the system dynamics—the frequency of the simple resonance excitation force ω is the bifurcation parameter, set $\zeta = 0.2$ and $R=0.8, b=0.05$, numerical simulation of the bifurcation phenomenon caused by the change of the system state with the frequency of the simple harmonic incentive force \dot{x} .

When the frequency of the harmonic incentive force \dot{x} changes within a certain range, the system has a stable period n-1 motion. However, as ω increases, the system will undergo period-doubling bifurcation, and eventually evolve into chaotic motion. And there are some period windows in the chaotic motion process, which is one of the typical characteristics of chaotic motion of nonlinear systems. With the further increase of ω , chaotic motion will degenerate into periodic motion [20]. When $c=2.65$, as shown in Figures 3.1 and 3.2, the phase plan of the system is not repeated but chaotic. At the same time, the irregular scattered point set in the Poincare cross section and the continuum in the spectrogram also indicate that the system is in chaotic motion. Figure 3 shows the chaotic attractor of the system on the Poincare section.

3.2. Design of chaos controller based on RBFNN. Since the chaotic motion is caused by the changes of some key parameters of the nonlinear dynamic system, based on this, this paper controls the chaotic motion based on the principle of the parameter feedback chaos control method. That is, the RBF neural network chaos controller outputs a small disturbance to the controllable parameters of the system, and the chaotic motion is controlled to the desired regular motion by dynamically adjusting the controllable parameters of the system [21]. When designing a chaos controller, the RBF neural network has a three-layer structure, including an input layer, a hidden layer and an output layer. According to the chaotic motion control target, two distances are taken as the inputs of the controller. One is the distance between the projection point on the Poincare section after K iterations, which can reflect the movement trend of the system approaching a stable period 1-1,

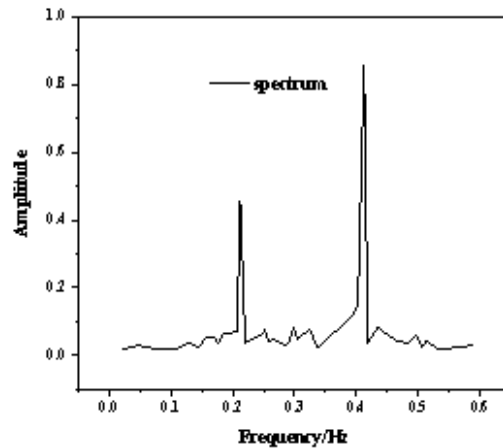


Fig. 3.2: Spectrogram of \dot{x}

and the projection point on the Poincare section after $k-1$ iterations. The other is the distance between the projection point on the Poincare section after $k-1$ iterations and the projection point on the Poincare section after $k-2$ iterations. The output of the controller is defined as the slight adjustment of the excitation frequency or damping coefficient of the system (that is, the small disturbance of the controller output is a controllable parameter applied to the system). Therefore, it is determined that the input layer of the RBF neural network has 2 nodes and the output layer is 1 node [22].

4. Results and analysis. The chaos control method proposed in this paper is used to control and simulate the chaotic attractor shown in Figure 3.1. The control method does not use the model information of the system. The model of the system is used in this paper to generate the input/output data of the system, and it is not used for the design of the controller [23].

The Gaussian RBF neural network is selected for chaos controller design, and after comparative analysis, it is found that when there are less than 5 hidden layer nodes, the simulation analysis finds that effective chaos control cannot be completed due to the weak nonlinear mapping ability of the controller. And when the hidden layer nodes increase, the nonlinear mapping ability of the controller will be enhanced, and the intelligent algorithm will be optimized to the appropriate controller parameters, and the control effect will become better [24].

However, with the further increase of hidden layer nodes, the control device structure will become more complicated, the controller parameters that need to be determined will also increase exponentially. It becomes more difficult for the intelligent algorithm to find the appropriate controller parameters, and the optimization efficiency of the algorithm decreases accordingly. According to the basic principle of determining the number of nodes in the hidden layer of the neural network (i.e., the network structure as compact as possible shall be selected under the premise of meeting the performance requirements of the control system, that is, the number of hidden layer nodes should be as few as possible), choose the least number of hidden layer nodes that can complete effective chaos control, that is, select 5 hidden layer nodes in the network. The parameters of the AHGSA algorithm are set as follows: the population size is 30, the maximum number of iterations is 100, $G_0 = 130$, $a=18$, and the proportional coefficient $p=0.96$. A small disturbance is applied to the controllable parameters of the system ω to suppress the chaotic motion of the system and make the system tend to a stable periodic motion [25]. In order to show the effect of chaotic motion control more clearly, the chaotic motion is controlled when the system is iterated for 400 times [26].

Figure 4.1 is a simulation result diagram of controlling chaotic motion into period 1-1 motion, showing

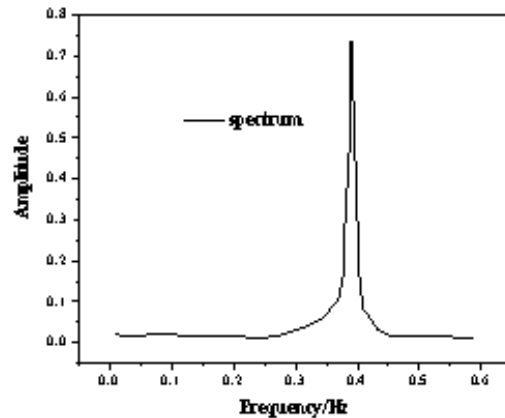


Fig. 4.1: Controlled period 1-1 motion of the system

Table 4.1: RBF neural network parameters (period 1-1)

Hidden layer node Center	Center width	Weights connecting hidden layer and output layer
-0.4644,0.0625	0.1552	-0.1294
0.0144,0.4323	0.4958	0.6095
0.3885,-0.1883	0.5481	0.6571
-0.4652,0.9523	0.9752	1.8718
0.1788,-0.4594	0.4056	-0.7668

the effect of chaotic motion control based on AHGSA-RBFNN. The parameters of the RBF neural network optimized by the AHGSA algorithm are shown in Table 4.1.

It can be seen from Figure 4.1 that the chaotic motion can be quickly controlled to a period of 1-1 motion, the phase diagram is a closed curve, and a peak appears in the spectrogram.

Figure 4.2 is the simulation result diagram of controlling chaotic motion into period 2-2 motion. The parameters of the RBF neural network optimized by the AHGSA algorithm are shown in Table 4.2.

It can be seen from Figure 4.3 that the chaotic motion can be quickly controlled to a period of 2-2 motion, the phase diagram is two closed curves, and the spectrogram shows two obvious peaks.

5. Conclusions. In this paper, RBF neural network for chaotic motion control of collision vibration system is proposed. The intelligent optimization control method based on RBF neural network is used to study the control of chaotic motion of a class of collision vibration system with gap. The Gaussian RBF neural network is selected for chaos controller design, and after comparative analysis, it is found that when there are less than 5 hidden layer nodes, due to the weak nonlinear mapping ability of the controller. Simulation analysis shows that effective chaos control cannot be completed. And when the hidden layer nodes increase, the nonlinear mapping ability of the controller is enhanced, and the intelligent algorithm is optimized to the appropriate controller parameters, and the control effect becomes better.

REFERENCES

- [1] Chen, D. , Li, S. , Wu, Q. , & Luo, X. . (2020). Super-twisting znn for coordinated motion control of multiple robot manipulators with external disturbances suppression. *Neurocomputing*, 371(Jan.2), 78-90.

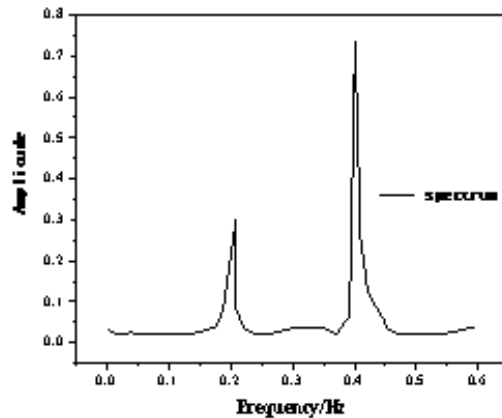


Fig. 4.2: RBF neural network parameters (period 2-2)

Table 4.2: RBF neural network parameters (period 1-1)

Hidden layer node Center	Center width	Weights connecting hidden layer and output layer
-0.5572,-0.0144	0.1552	- 0.4047
-0.4342,-0.2694	0.2271	1.4517
0.6567,- 0.2487	0.1656	1.1381
-0.4286 -0.0285	0.4051	0.1678
-0.3258,- 0.5973	0.3731	-1.1045

[2] Perez, & Humberto, J. . (2016). Neural control for synchronization of a chaotic chua-chen system. *IEEE Latin America Transactions*, 14(8), 3560-3568.

[3] Hu, C. , Ou, T. , H Chang, Yu, Z. , & Zhu, L. M. . (2020). Deep gru neural-network prediction and feedforward compensation for precision multi-axis motion control systems. *IEEE/ASME Transactions on Mechatronics*, PP(99), 1-1.

[4] Hsiao, F. H. . (2016). Neural-network based approach on delay-dependent robust stability criteria for dithered chaotic systems with multiple time-delay. *Neurocomputing*, 191(may 26), 161-174.

[5] Huynh, T. T. , Le, T. L. , & Lin, C. M. . (2019). Self-organizing recurrent wavelet fuzzy neural network-based control system design for mimo uncertain nonlinear systems using topsis method. *International Journal of Fuzzy Systems*, 21(2), 468-487.

[6] Burdukovskiy, I. , Kaneko, J. , & Horio, K. . (2015). Configuration method of fixing system with 2-dimensionally low-frequency vibration for drilling to decrease influence from unintended displacement of workpiece. *International Journal of Automation Technology*, 9(2), 161-169.

[7] Jaddi, N. S. , & Abdullah, S. . (2018). Optimization of neural network using kidney-inspired algorithm with control of filtration rate and chaotic map for real-world rainfall forecasting. *Engineering Applications of Artificial Intelligence*, 67(jan.), 246-259.

[8] Xu, Z. , Li, S. , Zhou, X. , Zhou, S. , & Cheng, T. . (2020). Dynamic neural networks for motion-force control of redundant manipulators: an optimization perspective. *IEEE Transactions on Industrial Electronics*, PP(99), 1-1.

[9] Lian, H. H. , Xiao, S. P. , Wang, Z. , Zhang, X. H. , & Xiao, H. Q. . (2019). Further results on sampled-data synchronization control for chaotic neural networks with actuator saturation. *Neurocomputing*, 346(JUN.21), 30-37.

[10] Balasubramaniam, P. , Muthukumar, P. , & Ratnavelu, K. . (2015). Theoretical and practical applications of fuzzy fractional integral sliding mode control for fractional-order dynamical system. *Nonlinear Dynamics*, 80(1-2), 249-267.

[11] Congxu, Zhu, Siyuan, Xu, Yuping, & Hu, et al. (2015). Breaking a novel image encryption scheme based on brownian motion and pwlem chaotic system. *Nonlinear Dynamics*, 79(2), 1511-1518.

[12] Qi, G. , & Chen, G. . (2015). A spherical chaotic system. *Nonlinear Dynamics*, 81(3), 1-12.

[13] Wang, H. , Wu, J. P. , Sheng, X. S. , Wang, X. , & Zan, P. . (2015). A new stability result for nonlinear cascade time-delay system and its application in chaos control. *Nonlinear Dynamics*, 80(1-2), 221-226.

[14] Fan, J. , Yu, Z. , Jin, H. , Wang, X. , D Bie, & Jie, Z. , et al. (2016). Chaotic cpg based locomotion control for modular self-reconfigurable robot. *Journal of Bionic Engineering*, 13(001), 30-38.

- [15] Zotos, & Euaggelos, E. . (2015). Classifying orbits in the restricted three-body problem. *Nonlinear Dynamics*, 82(3), 1233-1250.
- [16] E Köse. (2016). Controller design by using non-linear control methods for satellite chaotic system. *Electrical Engineering*, 99(2), 1-11.
- [17] Zeng, H. B. , Teo, K. L. , He, Y. , Xu, H. , & Wang, W. . (2017). Sampled-data synchronization control for chaotic neural networks subject to actuator saturation. *Neurocomputing*, 185(oct.18), 1656-1667.
- [18] Kong, L. , Li, D. , Zou, J. , & He, W. . (2020). Neural networks-based learning control for a piezoelectric nanopositioning system. *IEEE/ASME Transactions on Mechatronics*, 25(6), 2904-2914.
- [19] Zeng, Z. P. , Liu, F. S. , Lou, P. , Zhao, Y. G. , & Peng, L. M. . (2016). Formulation of three-dimensional equations of motion for train–slab track–bridge interaction system and its application to random vibration analysis. *Applied Mathematical Modelling*, 40(11-12), 5891-5929.
- [20] Amer, & Y., A. . (2015). Resonance and vibration control of two-degree-of-freedom nonlinear electromechanical system with harmonic excitation. *Nonlinear Dynamics*, 81(4), 2003-2019.
- [21] Huang, X. , Su, Z. , & Hua, H. . (2018). Application of a dynamic vibration absorber with negative stiffness for control of a marine shafting system. *Ocean Engineering*, 155(MAY 1), 131-143.
- [22] Kim, H. S. , Chang, C. , & Kang, J. W. . (2015). Evaluation of microvibration control performance of a smart base isolation system. *International Journal of Steel Structures*, 15(4), 1011-1020.
- [23] Saeed, N. A. , & Kandil, A. . (2019). Lateral vibration control and stabilization of the quasiperiodic oscillations for rotor-active magnetic bearings system. *Nonlinear Dynamics*, 98(2), 1191-1218.
- [24] Tavakoli, M. M. , & Assadian, N. . (2018). Predictive fault-tolerant control of an all-thruster satellite in 6-dof motion via neural network model updating. *Advances in Space Research*, 61(6), 1588-1599.
- [25] Mezyk, A. , Klein, W. , Pawlak, M. , & Kania, J. . (2017). The identification of the vibration control system parameters designed for continuous miner machines. *International Journal of Non-Linear Mechanics*, 91(MAY), 181-188.
- [26] Johnston, D., N., Plummer, A., & R., et al. (2017). Performance analysis of an energy-efficient variable supply pressure electro-hydraulic motion control system (retraction of vol 48, pg 10, 2016). *Control engineering practice*, 60, 193-193.

Edited by: B Nagaraj M.E.

Special issue on: Deep Learning-Based Advanced Research Trends in Scalable Computing

Received: Dec 6, 2023

Accepted: Feb 6, 2024